Pure Appl. Chem., Vol. 81, No. 9, pp. 1569–1584, 2009.
doi:10.1351/PAC-CON-08-10-02

Surface complexation and proton-promoted dissolution in aqueous apatite systems*

Åsa Bengtsson and Staffan Sjöberg‡

Department of Chemistry, Umeå University, S-90187 Umeå, Sweden

Abstract: The dissolution of hydroxyapatite (HAP) and fluorapatite (FAP) has been studied (25 °C, 0.1 M NaCl medium) within the pH ranges 2–11 (FAP) and 4–10 (HAP). A range of techniques has been utilized to achieve understanding in how these two abundant minerals may interact with their natural surroundings (e.g., body fluids and soil environments). Synthetic crystalline HAP and FAP were prepared, and both minerals were found to undergo a phase transformation generated during a dialysis step of the synthetic routes. Surface-deficient layers with the nonstoichiometric compositions $Ca_{8.4}(HPO_4)_{1.6}(PO_4)_{4.4}(OH)_{0.4}$ and $Ca_9(HPO_4)_2(PO_4)_4F_2$ were identified. The equilibrium analysis of experimental solubility data of the two apatite systems was based upon potentiometric titration data, batch experiments, and zeta-potential measurements in combination with information provided by X-ray photoelectron spectroscopy (XPS) and attenuated total reflectance-Fourier transform infrared (ATR-FTIR) spectroscopy. The analysis required, besides the two solubility equilibria, the formation of surface protonation/deprotonation reactions, re-adsorption processes involving phosphate and fluoride ions as well as an ion exchange reaction ($\equiv F + H_2O \leftrightharpoons \equiv OH + H^+ + F^-$) to fully describe the dissolution characteristics of the two apatite systems. The resulting model also agrees with observations from XPS and solubility data, claiming the formation of $CaF_2(s)$ in the most acidic pH range of the FAP system. In addition, calculated isoelectric points (pH_{iep}) are in agreement with values from surface charge measurements showing pH_{iep} (HAP) = 8.1 and pH_{iep} (FAP) = 5.7.

Keywords: fluorapatite; hydroxyapatite; phase transformation; spectroscopy; surface complexation modeling.

INTRODUCTION

Phosphorus (P) is an element critical for life. The cycling of P in soils, sediments, and aquifers has been the object of many studies in the contexts of fertilization and also, more lately, eutrophication [1,2]. An excess of P causes environmental problems in both fresh water and marine ecosystems. A recent example is the overabundance of P in the Baltic Sea that triggers rapid growth of aquatic plants, algae, and bacteria, in particular, huge blooms of blue–green cyano bacteria causing oxygen-depleted bottom waters [3]. This in turn causes the death of plankton and fish, destroying the food chain. A challenge to the scientific community is to find ways of remediating natural waters rich in P. One obvious way (though not easy to facilitate in huge water masses) is to precipitate or adsorb phosphate ions into bottom sediments. However, a recent calculation [4] shows a depletion of known P reserves before the end

*Paper based on a presentation at the 13th International Symposium on Solubility Phenomena and Related Equilibrium Processes (ISSP-13), 27–31 July 2008, Dublin, Ireland. Other presentations are published in this issue, pp. 1537–1614.

‡Corresponding author: Fax: + 46 90 786 9195; E-mail: staffan.sjoberg@chem.umu.se

of this century. Certainly, it therefore sounds foolish to dump an element critical for life at the bottom of lakes and seas.

The excess of P originates from the weathering of phosphate-containing minerals, phosphate fertilizers, human sewage, and detergents. Apatites [$Ca_5(PO_4)_3(F,Cl,OH)$] are the most common P-bearing minerals in nature. Of these, fluorapatite (FAP) is the most abundant. It is present in almost all igneous rocks, typically comprising 0.1–1 vol %. Apatite is also found extensively in sedimentary deposits, called phosphorites, which can contain up to 80 % of apatite and is often interbedded with limestone.

Weathering of apatites is the initial source of P to the global system. Released phosphate is very reactive and can, besides forming soluble complexes with cations, precipitate with, for example, Ca, Mg, Fe, Al, and Mn in soils. It can also strongly adsorb to surfaces of different metals (oxo)hydroxide of Fe(III), Al(III), Mn(III,IV), like goethite (α-FeOOH), gibbsite [α-$Al(OH)_3$], manganite (γ-MnOOH), and pyrolusite (β-MnO_2), as well as to organic matter in soils.

Phosphate is very immobile in most soils and is not necessarily directly bioavailable for plant uptake. However, plants and microorganisms have developed different strategies to increase their supply of P. They can, for example, secrete an enzyme, phosphatase, which cleaves inorganic phosphates from organophosphates. They can also exude small organic acids such as malonic acid and citric acid [5]. These acids can affect the amount of bioavailable phosphate in several different ways: (i) they cause a decrease in pH which enhances the dissolution of minerals like apatite, (ii) they take part in processes such as complexation with Ca which also will cause an increase in apatite solubility, and (iii) the acids can also out-compete phosphate that is adsorbed to different mineral surfaces and make phosphate more easily bioavailable.

Apatite is also the most important Ca phosphate mineral occurring in the human body. A carbonate-containing Ca-deficient apatite is a major component of bones and teeth, and as hydroxyapatite (HAP) is very similar to this component, synthetic HAP is a promising material for artificial bone and teeth implants [6].

Bones are always in contact with surrounding extra-cellular fluids and are therefore very susceptible to the content of the fluid. For example, toxic elements like Cd and Pb that are introduced to extracellular fluids can potentially accumulate in bones. Bones also provide a reservoir of Ca, phosphate, and carbonate ions to the extra-cellular fluids, and the solubility of the bone mineral controls the concentration of these ions [7]. Dallemagne and Richelle [8] discovered that bones contain 0.8–0.9 wt % citrate that is likely to be adsorbed onto apatite crystals of bones. This citrate most likely influences the solubility of the bone mineral and therefore also changes the composition of the extra-cellular fluid.

Bacteria in the mouth produce acids that attack the teeth and cause tooth decay. Fluoridation of apatite in teeth is believed to suppress tooth decay, and the role of the fluoride ions in this process has been the subject of numerous investigations [9–11]. Precipitation of less-soluble FAP, formation of protective surface layers containing fluoride ions, and inhibition of acid generation from oral bacteria are some suggestions for why fluoride suppresses dental decay. The role of fluoride ions in enamel caries, however, seems to be far from understood.

The objective of the present paper is to present new results [12,13] related to the surface chemistry of apatites with particular emphasis on the design of equilibrium models that include not only solubilities but also complexation in solution and at the mineral–water interface.

APATITE SYNTHESIS AND SUSPENSION CHARACTERISTICS

HAP was synthesized according to a method modified from Hayek and Stadlmann [14]. A 1600-ml solution of 0.37 M $(NH_4)_2HPO_4$ (Merck) was adjusted to pH 12 by adding small portions of NH_3 (Scharlau). This solution was added drop-wise to a 1200-ml solution of 0.83 M $Ca(NO_3)_2\,4H_2O$ (Schaurlau) (also adjusted to pH 12 by additions of NH_3). FAP was synthesized according to the method

by Penel et al. [15]. A solution of 1000 ml of 0.4 M $Ca(NO_3)_2{\cdot}4H_2O$ was added drop-wise to a boiling solution of 1000 ml 0.24 M $(NH_4)_2HPO_4$ and 0.18 M NH_4F (Merck) over a 1-h period. Solution pH was kept to a value of about 9 by addition of small aliquots of 25 % NH_3 (Scharlau). The HAP/FAP products were matured for 1 h at approximately 80 °C and then cooled to room temperature. Excess ions were removed by repeated washes several times with deionized and boiled water and finally with a three-month dialyses period (Millipore 12-14000 D tubes). The precipitate was then dried at room temperature, gently mortared, and stored in polyethene bottles.

The products were characterized by X-ray diffraction (XRD) and were found to produce patterns characteristic of HAP and FAP. The elemental composition of the bulk was analyzed by Analytica AB, Luleå, Sweden, using inductively coupled plasma-atomic emission spectrometry (ICP-AES) or sector field mass spectrometry (ICP-SFMS), and the Ca/P ratio was found to be 1.6 for HAP and 1.7 for FAP. The specific surface area was measured by the BET (N_2) single-point method using a Micrometrics Flowsorb II 2300 and was determined to be 80.5 m^2/g (HAP) and 10.7 m^2/g (FAP).

The reaction times necessary to reach equilibrium amounted to approximately three months. This was obvious from a series of batch experiments in which pH was measured with time. As HAP and FAP both are basic minerals releasing PO_4^{3-} ions (and OH^- for HAP) pH_0 (equilibrium pH of the suspension in the absence of excess acid or base) of the suspensions are expected to be above 7 and the actual pH reflects the apatite solubility. It is interesting to note that this is the case for HAP but not for FAP. The typical value for HAP is ≈8.0 , while a suspension of FAP generates pH values in the slightly acidic range!

SURFACE CHARACTERIZATIONS

Surface site compositions

It has been suggested that apatites form surface layers of different compositions than the bulk when they get in contact with an aqueous solution [16–18], but the composition of these surface layers is not fully understood. What is clear is that the formation of a surface layer would affect the solubility of the mineral and that the solubility would reflect the composition of the surface layer and not the apatite in the bulk. One process that has been suggested to be responsible for the formation of this nonstoichiometric surface layer on HAP is the creation of vacancies on Ca and OH sites and the protonation of phosphate groups. The range of composition may be expressed as $Ca_{(10-x)}(HPO_4)_x(PO_4)_{(6-x)}(OH)_{(2-x)}$, but the limiting composition of this nonstoichiometric HAP is somewhat uncertain. Limiting values of $x = 1$ [$Ca_9HPO_4(PO_4)_5OH$, with Ca/P = 1.5] [10], $x = 2$ [$Ca_8(HPO_4)_2(PO_4)_4$ with Ca/P = 1.33] [19] as well as 1.4 with a surface composition of [$Ca_{8.4}(HPO_4)_{1.6}(PO_4)_{4.4}(OH)_{0.4}$] [20], have been suggested.

It thus seems important to characterize these surface layers in order to be able to interpret not only surface complexation reactions, but also the dissolution processes.

The protolytic surface properties of HAP particles are assumed to be controlled by different phosphate and calcium hydroxyl sites. In a recent work [21], the active P surface sites as well as bulk phosphate of FAP was characterized using single-pulse ^1H, ^{31}P, and ^{31}P MAS NMR. The surface sites were defined as $\equiv PO_x$, $\equiv PO_xH$, and $\equiv PO_xH_2$ with $x = 1$, 2, or 3 (charges omitted). This defines the unprotonated sites $\equiv O_3PO$, $\equiv O_2PO_2^-$, and $\equiv OPO_3^{2-}$ and a number of possible protonated ($\equiv O_2PO_2H$, $\equiv OPO_3H^-$, and $\equiv PO_3H_2$) sites. (The formation of positively charged phosphate sites is assumed to be less likely.) The ^{31}P MAS NMR spectrum of FAP at a pH of 5.9 (close to $pH_{iep} = 5.7$) showed one dominating resonance line at 2.9 ppm, which was ascribed to bulk phosphate groups and two weaker shoulder peaks at 5.4 and 0.8 ppm, respectively, corresponding to the unprotonated and protonated surface sites. The presence of the latter has moreover been confirmed with vibration spectroscopy [12]. A resonance peak at –4.5 ppm also appeared at a pH of 3.5 from a $\equiv PO_xH_2$ surface species (most likely $\equiv OPO_3H_2$ at this low pH value). In conclusion, these results reveal the formation of protonated and un-

protonated phosphate-containing surface sites, with a relative ratio that is affected by pH. These measurements did not, however, provide any information on the specific surface charge of these sites.

The protolytic properties of Ca sites at the surface of synthetic FAP particles have been studied using ^{1}H and ^{31}P MAS NMR methods [22]. Three possible forms of Ca hydroxyl sites were suggested, viz. $\equiv CaOH_2^+$, $\equiv CaOH$, and $\equiv Ca(OH)_2^-$. Furthermore, their mutual ratios were found to vary with pH.

Surface site concentrations

Radioisotope determination of the surface concentrations of Ca and P on stoichiometric (Ca/P = 1.67) HAP, which was aged for about one month in aqueous solution ($I \approx 0$), has been performed by Kukura et al. [16]. The areas per PO_4^{3-} and Ca^{2+} ion at the point of zero charge (pH = 8.5) were found to be 33.1 ± 2.7 and 23.0 ± 2.1 Å^2. The calculated area (based upon crystallographic data) per P atom is 32.4 Å^2 and for Ca is 19.5 Å^2. It can thus be noted that the Ca/P ratio obtained from crystallographic data and bulk analysis was 1.67, whereas the isotope measurements give a surface ratio of 1.44. This lower value suggests that a phase transformation of the surface has occurred and that the new surface layer consists of a Ca-deficient phase. It was also found that the additions of Na^+, K^+, and Cl^- ions had no significant effect on the area per P or Ca, indicating that the adsorption and/or exchange reactions (Ca^{2+}/Na^+,K^+; PO_4^{3-}/Cl^-) can be neglected. This has also been confirmed in other studies [23,24].

From the radioisotope measurements by Kukura et al. [16], site densities (N_s) of 3.0 of phosphate and 4.3 sites/nm^2 of Ca were obtained. These values can be compared with values obtained from alkalimetric titrations of synthetic carbonate-free FAP by Jarlbring et al. [25]. They found N_s to be 2.95 sites/nm^2 and 2.34 sites/nm^2 of hydroxide reactive sites in ionic strengths of 0.1 and 0.5 M $NaNO_3$, respectively. A corresponding alkalimetric titration by Perrone et al. [26] obtained N_s = 3.1 sites/nm^2 for synthetic carbonate FAPs. They also assumed the surface site to show amphoteric properties, which means that a total of 6.2 (3.1 + 3.1) sites/nm^2 could be reacted. As the numbers of sites based on the radioisotope measurements by Kukura et al. [16] are in close agreement with those of Jarlbring et al. [25] and Perrone et al. [26] they were chosen for the model calculations of this study.

Solution speciation

Apatites are complex minerals, and when investigating their dissolution a number of possible side reactions must be taken into account. The dissolution according to reactions 1 and 2 are strongly pH-dependent and coupled with protonation and complexation reactions like those of 3 and 4. For FAP, complexation reactions involving the fluoride ion (reactions 5 and 6), as well as the formation of a secondary precipitate at low pH (reaction 7), also have to be considered:

$$Ca_5(PO_4)_3OH(s) \leftrightharpoons 5Ca^{2+} + 3PO_4^{3-} + OH^- \quad (1)$$

$$Ca_5(PO_4)_3F(s) \leftrightharpoons 5Ca^{2+} + 3PO_4^{3-} + F^- \quad (2)$$

$$PO_4^{3-} + nH^+ \leftrightharpoons H_nPO_4^{(3-n)-} \quad (n = 1, 2, 3) \quad (3)$$

$$Ca^{2+} + PO_4^{3-} + nH^+ \leftrightharpoons CaH_nPO_4^{(n-1)+} \quad (n = 1, 2) \quad (4)$$

$$Ca_5(PO_4)_3F(s) + 6H^+ \leftrightharpoons CaF^+ + 4Ca^{2+} + 3H_2PO_4^- \quad (5)$$

$$nF^- + H^+ \leftrightharpoons HF_n^{(2n-1)+} \quad (n = 1, 2) \quad (6)$$

$$Ca^{2+} + 2F^- \leftrightharpoons CaF_2\,(s) \quad (7)$$

Surface speciation

The adsorption of H^+ and OH^- ions as well as the possible re-adsorption of Ca and/or phosphate and fluoride species during the dissolution process will be described assuming the presence of three reactive surface sites, viz ≡CaOH, $\equiv OPO_3H_2$, and ≡F. This is, of course, a simplification but is justified by the approach of describing experimental data with a surface complexation model including as few parameters as possible. From these sites, the following type of general equilibria will be considered:

$$\equiv CaOH + nH^+ \leftrightharpoons \equiv CaOH_{n+1}^{\,n+} \qquad (n = -1, 1) \tag{8}$$

$$\equiv OPO_3H_2 \leftrightharpoons \equiv OPO_3H_{2-n}^{\,n-} + nH^+ \qquad (n = 1, 2) \tag{9}$$

$$\equiv CaOH_2^{\,+} + H_2PO_4^{\,-} \leftrightharpoons \equiv CaOPO_3H_n^{\,(n-2)-} + (2-n)\,H^+ + H_2O \qquad (n = 0, 1, 2) \tag{10}$$

$$\equiv OPO_3^{\,2-} + Ca^{2+} + nH^+ \leftrightharpoons \equiv OPO_3H_nCa^{n+} \qquad (n = 0, 1, 2) \tag{11}$$

$$\equiv OPO_3H_2 + Na^+ \leftrightharpoons \equiv OPO_3H_{2-n}\,Na^{(1-n)+} + nH^+ \qquad (n = 1, 2) \tag{12}$$

$$\equiv F + H_2O \leftrightharpoons \equiv OH + H^+ + F^- \tag{13}$$

$$\equiv CaOH_2^{\,+} + F^- \leftrightharpoons \equiv CaF + H_2O \tag{14}$$

The number of reactions presented above demonstrates the complexity of apatite dissolution, and due to this complexity it is crucial to make use of a wide range of analytical techniques when trying to elucidate these processes. Most studies on this subject have, however, only analyzed ions dissolved from the apatites and not investigated mineral surfaces. In this work we have used batch experiments, potentiometric titrations, zeta-potential measurements, and XPS and ATR-FTIR spectroscopy and combined the results from these analyses to create one complete model of the dissolution of HAP and FAP over a large pH interval.

Surface complexation modeling

Surface complexation models can be used to describe reactions taking place at the interface between a mineral and a solution.

The formation of a number of charged surface species acc. to reactions 8–12 will result in a charge accumulation at the mineral surface. Therefore, the different surface equilibrium constants must be corrected for the coulombic energy of the charged surface.

The conditional constant, $\beta^s{}_{11}$(cond.) defining a protonation reaction of a generic surface site ≡SOH:

$$\equiv SOH + H^+ \leftrightharpoons \equiv SOH_2^{\,+} \tag{15}$$

is related to the intrinsic constant $\beta^s{}_{11}$(intr.) according to the equation

$$\beta^s{}_{11}(\text{intr.}) = \beta^s{}_{11}(\text{cond.})\, e^{F\Psi/RT} \tag{16}$$

where Ψ is the acting surface potential calculated according to equation 17

$$\Psi = T_\sigma \cdot F/(s \cdot A \cdot C) \tag{17}$$

where Ψ is the surface potential (V), C is a constant with the dimensions of specific capacitance (CV^{-1}/m^2), T_σ is the molarity of total surface charge (mol/l), s is the specific surface area (m^2/g), and A is the solid concentration (g/l). The models used in the present work are developed assuming a constant capacitance for the electrical double layer at the charge surface. The surface acid/base properties of HAP and FAP will be described with the constant capacitance model (CCM) [27]. Even though more sophisticated models could be built, we chose to work with the simpler CCM model due to the com-

plexity of these multicomponent systems. In this model, adsorbed ions are assumed to be directly bound to the surface and no distinction is made between inner- and outer-sphere complexes.

EQUILIBRIUM ANALYSIS: STRATEGY

The strategy in modeling surface complexation and dissolution of HAP and FAP is to yield information provided by different macroscopic techniques: (i) potentiometric measurements generating H(pH) data; (ii) dissolution characteristics with respect to soluble total concentrations of Ca, phosphate, and fluoride; and (iii) surface charge measurements to identify pH_{iep}. Furthermore, this information is combined with surface spectroscopic data from XPS, FTIR, and NMR measurements. The presentation will highlight similarities and differences found in the HAP and FAP systems.

Adsorption studies of Ca in different metal (hydr)oxide systems have shown Ca to become adsorbed in neutral/alkaline solutions [28,29]. Furthermore, possible re-adsorption of phosphate anions are more likely to take place to positively charged surfaces in acidic to neutral solutions than in alkaline solutions. This is also corroborated by a number of studies on phosphate adsorption in metal(hydr)oxide systems [29–32].

The equilibrium model shown in Table 1 is defined by the 8 components: H^+, Ca^{2+}, Na^+, HPO_4^{2-}, F^-, ≡CaOH, $\equiv OPO_3H_2$, and ≡F. A general equilibrium reaction for FAP can be written as given by

$$p\mathrm{H^+} + q\mathrm{Ca^{2+}} + r\mathrm{Na^+} + s\mathrm{HPO_4^{2-}} + t\mathrm{F^-} + u \equiv\mathrm{CaOH} + v \equiv\mathrm{OPO_3H_2} + x \equiv\mathrm{F} \leftrightharpoons (\mathrm{H^+})_p(\mathrm{Ca^{2+}})_q(\mathrm{Na^+})_r(\mathrm{HPO_4^{2-}})_s(\mathrm{F^-})_t(\equiv\mathrm{CaOH})_u(\equiv\mathrm{OPO_3H_2})_v(\equiv\mathrm{F})_x \quad (18)$$

This equation defines the formation constant $\beta_{pqrstuvx}$.

The total concentration of the different components is obtained by summarizing within the different columns in Table 1, viz.

$$[\mathrm{H^+}]_{tot} = [\mathrm{H^+}]_{tot}(\mathrm{sln}) + [\mathrm{H^+}]_{tot}(\mathrm{srfc}) + [\mathrm{H^+}]_{tot}(\mathrm{sld}) = [\mathrm{H^+}] - [\mathrm{OH^-}] - [\mathrm{PO_4^{3-}}] + [\mathrm{H_2PO_4^-}] + 2\,[\mathrm{H_3PO_4}] - [\mathrm{Ca(OH)^+}] - [\mathrm{Ca(PO_4)^-}] + [\mathrm{Ca(H_2PO_4)^+}] + [\mathrm{HF}] + [\mathrm{HF_2^-}] + [\equiv\mathrm{CaOH_2^+}] - [\equiv\mathrm{PO_4H^-}] - 2[\equiv\mathrm{OPO_3Na^-}] + [\equiv\mathrm{CaOPO_3H^-}] + [\equiv\mathrm{CaF}] - [\equiv\mathrm{OH}] - 4n(\mathrm{Ca_9(HPO_4)_2(PO_4)_4(F)_2}) - 4.8n[\mathrm{Ca_{8.4}(HPO_4)_{1.6}(PO_4)_{4.4}(OH)_{0.4}}] \quad (19)$$

Here, n denotes the number of moles of the solid phases per litre solution. In the experiments, acid (H^+) or base (OH^-) has been added. This equation shows that these additions will be consumed due to (i) dissolution of FAP, (ii) surface complexation reactions, as well as (iii) complexation in solution. In addition to these data, the total concentration of Ca, phosphate, and fluoride in solution is known from chemical analysis. These experimental values can also be compared with model-dependent calculated values, which can be derived from Table 1.

$$[\mathrm{Ca^{2+}}]_{tot}(\mathrm{sln}) = [\mathrm{Ca^{2+}}] + [\mathrm{Ca(OH)^+}] + [\mathrm{Ca(PO_4)^-}] + [\mathrm{Ca(HPO_4)}] + [\mathrm{Ca(H_2PO_4)^+}] \quad (20)$$

$$[\mathrm{HPO_4^{2-}}]_{tot}(\mathrm{sln}) = [\mathrm{PO_4^{3-}}] + [\mathrm{HPO_4^{2-}}] + [\mathrm{H_2PO_4^-}] + [\mathrm{H_3PO_4}] + [\mathrm{Ca(PO_4)^-}] + [\mathrm{Ca(HPO_4)}] + [\mathrm{Ca(H_2PO_4)^+}] \quad (21)$$

$$[\mathrm{F^-}]_{tot}(\mathrm{sln}) = [\mathrm{F^-}] + [\mathrm{HF}] + 2\,[\mathrm{HF_2^-}] + [\mathrm{CaF^+}] \quad (22)$$

In the different model calculations error squares of sums (U):

$$U(\mathrm{H}) = \sum ([\mathrm{H^+}]_{tot}^{calc} - [\mathrm{H^+}]_{tot}^{exp})^2 \quad (23)$$

$$U(\mathrm{Ca}) = \sum ([\mathrm{Ca^{2+}}]_{tot}(\mathrm{sln})^{calc} - [\mathrm{Ca^{2+}}]_{tot}(\mathrm{sln})^{exp})^2 \quad (24)$$

$$U(\mathrm{P}) = \sum ([\mathrm{HPO_4^{2-}}]_{tot}(\mathrm{sln})^{calc} - [\mathrm{HPO_4^{2-}}]_{tot}(\mathrm{sln})^{exp})^2 \quad (25)$$

$$U(F) = \sum ([F^-]_{tot}\,(sln)^{calc} - [F^-]_{tot}\,(sln)^{exp})^2 \quad (26)$$

were used in fitting a model to experimental $[H^+]_{tot}$, $[Ca^{2+}]_{tot}$ (sln), $[HPO_4^{2-}]_{tot}$ (sln), and $[F^-]_{tot}$(sln) data. The ultimate goal of the equilibrium analysis is to design a model that gives a good fit to U(H) + U(Ca) + U(P) + U(F). This analysis involves a determination of composition and stability of the FAP phase as well as the prevailing surface complexes. It is assumed that literature data describing complexation in solution is known, and no attempts will be made to refine any of the solution complexation constants. It is also assumed that the surface complexation constants for reactions 8–12 are the same as in the HAP system [12]. This means that the number of unknown parameters will be limited to the solubility product for FAP, ion exchange, and re-adsorption equilibria involving fluoride ions as well as a capacitance value. Reaction 18 and eqs. 19–25 are also valid for the HAP system when the fluoride species in Table 1 are excluded from the calculations.

Table 1 Thermodynamic data (I = 0.1 M; 25 °C) used in the model calculations. sln, srfc, and sld stand for solution, surface, and solid, respectively. The "best" fitting capacitance values were 1.3 and 3.4 CV^{-1}/m^2 for HAP and FAP, respectively.

Species	Log β	H^+	Ca^{2+}	HPO_4^{2-}	Na^+	F^-	≡CaOH	$\equiv OPO_3H_2$	≡F	Phase
H^+	0	1	0	0	0	0	0	0	0	sln
Ca^{2+}	0	0	1	0	0	0	0	0	0	sln
HPO_4^{2-}	0	0	0	1	0	0	0	0	0	sln
Na^+	0	0	0	0	1	0	0	0	0	sln
F^-	0	0	0	0	0	1	0	0	0	sln
≡CaOH	0	0	0	0	0	0	1	0	0	srfc
$\equiv OPO_3H_2$	0	0	0	0	0	0	0	1	0	srfc
≡F	0	0	0	0	0	0	0	0	1	srfc
OH^-	–13.78	–1	0	0	0	0	0	0	0	sln
PO_4^{3-}	–11.65	–1	0	1	0	0	0	0	0	sln
$H_2PO_4^-$	6.74	1	0	1	0	0	0	0	0	sln
H_3PO_4	8.65	2	0	1	0	0	0	0	0	sln
$Ca(OH)^+$	–12.9	–1	1	0	0	0	0	0	0	sln
$Ca(PO_4)^-$	–6.45	–1	1	1	0	0	0	0	0	sln
$Ca(HPO_4)$	1.73	0	1	1	0	0	0	0	0	sln
$Ca(H_2PO_4)^+$	7.32	1	1	1	0	0	0	0	0	sln
HF	2.92	1	0	0	0	1	0	0	0	sln
HF_2^-	3.51	1	0	0	0	2	0	0	0	sln
CaF^+	0.82	0	1	0	0	1	0	0	0	sln
$\equiv OPO_3H^-$	–1.11	–1	0	0	0	0	0	1	0	srfc
$\equiv OPO_3Na^-$	–11.08	–2	0	0	1	0	0	1	0	srfc
$\equiv CaOH_2$	$^+$8.41	1	0	0	0	0	1	0	0	srfc
$\equiv CaOPO_3H^-$	11.63	1	0	1	0	0	1	0	0	srfc
≡CaF	11.40	1	0	0	0	1	1	0	0	srfc
≡OH	–8.78	–1	0	0	0	–1	0	0	1	srfc
$Ca_{8.4}(HPO_4)_{1.6}(PO_4)_{4.4}(OH)_{0.4}$[a]	23.27	–4.8	8.4	6	0	0	0	0	0	sld
$Ca_9(HPO_4)_2(PO_4)_4(F)_2$[a]	48.08	–4	9	6	0	2	0	0	0	sld
CaF_2	9.73	0	1	0	0	2	0	0	0	sld

[a]The solid phase included is the composition of the surface layers of HAP [12] and FAP [13]. All constants, except those for the surface complexation model, were taken from Smith and Martell [32]. The surface complexes were taken from Bengtsson et al. [12,13].

The strategy of the equilibrium analysis will be determinations of:

(i) An initial approximate value of the solubility product of HAP and FAP minimizing U(Ca) and U(P) using data where the dissolution reaction is predominating (pH ≤ 5). In these calculations the high solubility will cause significant changes of the ionic strengths which are corrected for in the calculations by using eq. 27. Composition of the solid phase will be obtained from XPS data together with an interpretation of solution analysis of the Ca/P ratio.

(ii) Composition and stability of surface protonation/deprotonation equilibria from the potentiometric titrations with pH ≥ pH_0. In these calculations the solubility product for HAP will be included in the calculations and U(H) will be minimized. Analysis of Ca and phosphate and fluoride released from HAP and FAP to the solution clearly showed that their solubility cannot be neglected even if pH = pH_0. This means that corrections for the proton uptake/release of soluble species (c.f. eqs. 3, 4, and 6, and the auto-protolysis of water) must be made when interpreting these surface complexation reactions.

(iii) Interpretation of possible re-adsorption constants (eq. 10) of phosphate anions in neutral to slightly acidic solutions minimizing U(Ca) + U(P).

(iv) By using an iterative procedure, constant obtained under (i), (ii), and (iii) will be refined, minimizing U(H) + U(Ca) + U(P) + U(F).

The activity coefficients of the different species in solution are controlled by an ionic medium of constant ionic strength (I = 0.1 M). In addition, the activity coefficients of the surface species were assumed to be constant. When necessary, the individual activity coefficients γ_i of an ionic species were recalculated to an ionic strength (I) of 0.1 utilizing Davis equation (eq. 11) [34], where z_i denotes the ionic charge number.

$$\log \gamma_i = -0.509 z_i^2 [I^{1/2}/(1 + I^{1/2}) - 0.3I] \quad (27)$$

In the different calculations, the computer code WinSGW [35], based on the SOLGASWATER algorithm [36] was used.

RESULTS

Surface composition of HAP and FAP

The two apatites were found to form surface layers that are compositionally different than the bulk. These surface layers formed in response from interfacial reactions with aqueous solutions during the dialysis procedure after the synthesis. As the solubility of mineral is reflected by the properties of surface layer(s), it becomes imperative that the composition of the surface layer(s) is known. In this section we present some of the results from investigations of the composition of the surface layers of the synthetic HAP and FAP. This information was then taken into account when calculating the dissolution and surface complexation behavior of the two apatites.

XPS was used to determine the composition of the surface layers formed on the HAP and FAP particles.

The results from these measurements (Fig. 1) confirm that the surfaces of the two minerals have a different composition than the one found for the bulk. For both minerals, the Ca/P ratios have decreased relative to the bulks. The HAP surface showed the composition with a Ca/P ratio of ~1.4 compared to the bulk + surface layer ratio of ~1.6, while the FAP surface showed the composition with a Ca/P ratio of ~1.5 compared to its bulk + surface layer with a ratio of 1.7. The Ca/P ratios on the two apatite surfaces were quite stable over a large pH interval, which supports the assumption of congruent dissolution reactions. The only major change was for the FAP surface at low pH. The samples equilibrated at pH < 4 reveal considerably lower Ca/F and P/F ratios and larger Ca/P ratios than those of the bulk material. These results reveal a preferential accumulation of both Ca and F at the surface of the

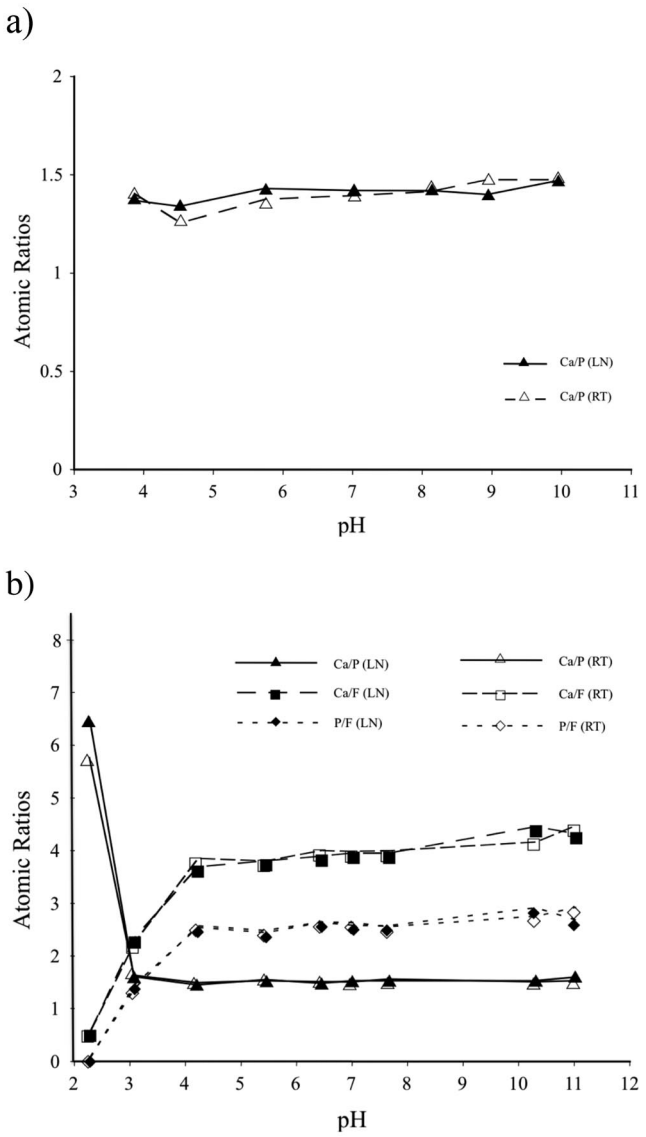

Fig. 1 Atomic ratios at the surfaces of (a) HAP and (b) FAP as a function of pH. The apatite suspension had been equilibrated for 3.5 months in 0.1 M Na(Cl) at 25 °C with a solid concentration of 7.7 g/l. The XPS analyses were performed both in room temperature (RT) and in liquid nitrogen (LN).

paste. Our thermodynamic calculations provide evidence that this enrichment is caused by the precipitation of CaF_2 (s). Furthermore, the FAP samples equilibrated in the pH 4–11 range reveal ratios of Ca/F = 3.9–4.5 and P/F = 2.5–2.9. This pH dependence on the surface composition of fluoride indicates a F^-/OH^- exchange reaction which causes the Ca/F and P/F ratios to increase slightly with increasing pH values.

Given the findings from XRD measurements confirming the apatite structures of the bulk, XPS data and the dissolution data, the two apatites are proposed to have surface layers with the compositions: $Ca_{8.4}(HPO_4)_{1.6}(PO_4)_{4.4}(OH)_{0.4}$ for HAP and $Ca_9(HPO_4)_2(PO_4)_4F_2$ for FAP.

Solubility of HAP and FAP

The data presented in Fig. 2 clearly show the differences in the dissolution between the two apatites. The concentration of Ca in solution is higher for HAP compared to FAP at pH values below 9, and the same relationship is valid for phosphate below pH 7. Above these pH values, the Ca and phosphate concentrations are comparable for both minerals. These results indicate that different processes are predominant under different pH conditions.

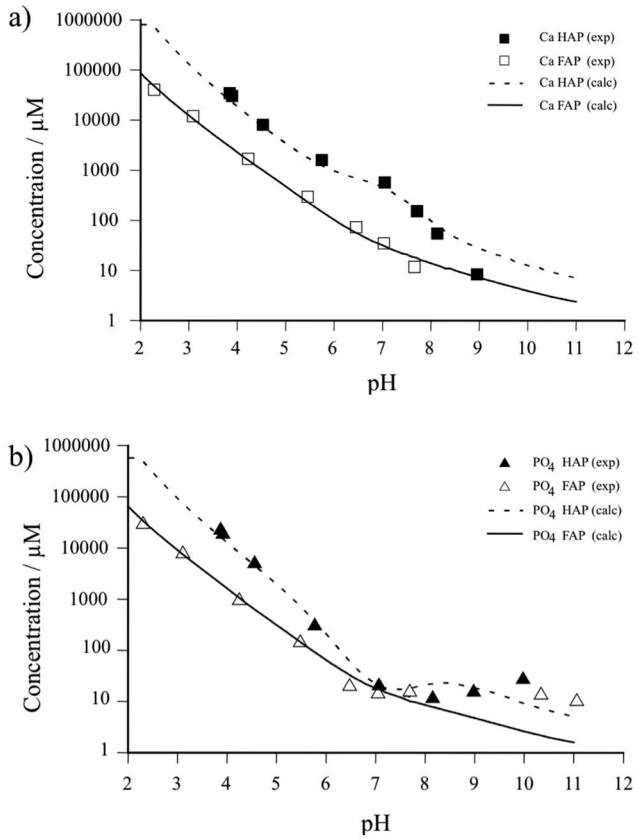

Fig. 2 Solubility of HAP and FAP illustrated by (a) Ca and (b) phosphate in solution. Lines are derived from model calculations (see below). The batches had been equilibrated for 3.5 months in 0.1 M Na(Cl) at 25 °C, and with a solid concentration of 7.7 g/l.

The predominating process in the most acidic suspensions (pH ≤ 5) is dissolution causing the concentrations of Ca and phosphate to amount up to 50 and 40 mM, respectively. By minimizing U(Ca) + U(P) preliminary formation constants for reactions 28 and 29 were obtained.

$$8.4Ca^{2+} + 6HPO_4^{2-} + 0.4H_2O \rightleftharpoons Ca_{8.4}(HPO_4)_{1.6}(PO_4)_{4.4}(OH)_{0.4}(s) + 4.8\ H^+ \quad (28)$$

$$9Ca^{2+} + 6HPO_4^{2-} + 2F^- \rightleftharpoons Ca_9(HPO_4)_2(PO_4)_4F_2(s) + 4H^+ \quad (29)$$

Surface complexation when pH ≥ pH_0

In the range pH ≥ pH_0 the predominating processes are surface protonation/deprotonation reactions, and they were investigated by potentiometric acid/base titrations of the minerals (Fig. 3).

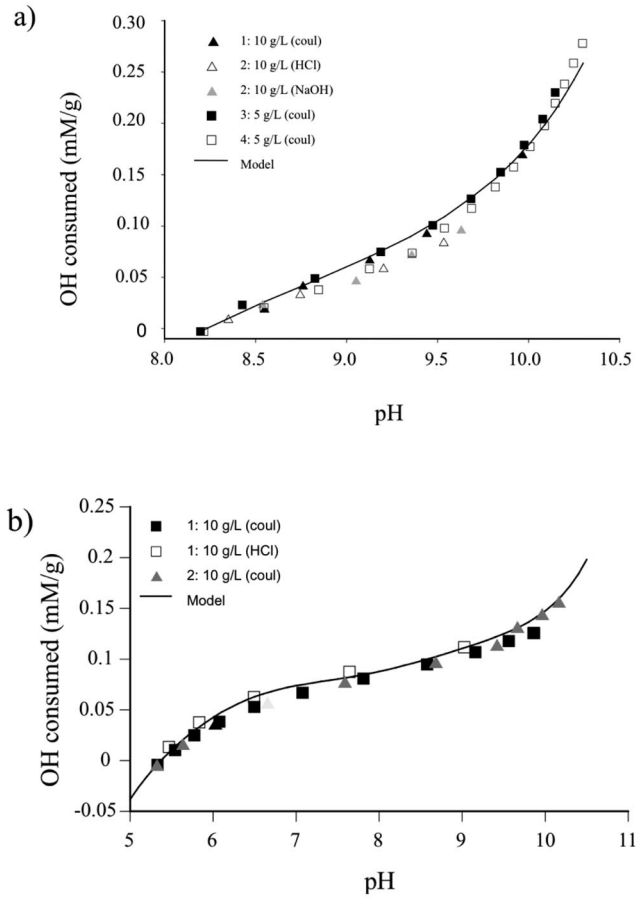

Fig. 3 Results of titration data of (a) HAP and (b) FAP suspensions. The solid concentration and method of titrant addition (coulometric, HCl, or NaOH) is specified in the legend. (I = 0.1 M Na(Cl) and T = 25 °C.)

The results from the titrations of HAP provided support for the surface reactions 30–33 [12]:

$$\equiv CaOH + H^+ \leftrightharpoons \equiv CaOH_2^+ \tag{30}$$

$$\equiv OPO_3H_2 \leftrightharpoons \equiv OPO_3H^- + H^+ \tag{31}$$

$$\equiv OPO_3H_2 + Na^+ \leftrightharpoons \equiv OPO_3Na^- + 2H^+ \tag{32}$$

The equilibrium analysis of the FAP system assumes that the intrinsic constants for the surface reactions related to the surface components ≡CaOH and $\equiv OPO_3H_2$ are the same for the Ca-depleted FAP surface as for the nonstoichiometric HAP (Table 1). In addition to equilibria in reactions 29–32, a reaction that accounts for quite high fluoride concentrations in solution had to be introduced

$$\equiv F + H_2O \leftrightharpoons \equiv OH + H^+ + F^- \tag{33}$$

This hypothesis is supported by the variation of pH and pF as a function of solid concentration visualized in Fig. 4. Both pH_0 and pF decrease with increasing solid concentration, which corroborates the theory of the ion-exchange reaction in which F^- and H^+ are released into solution.

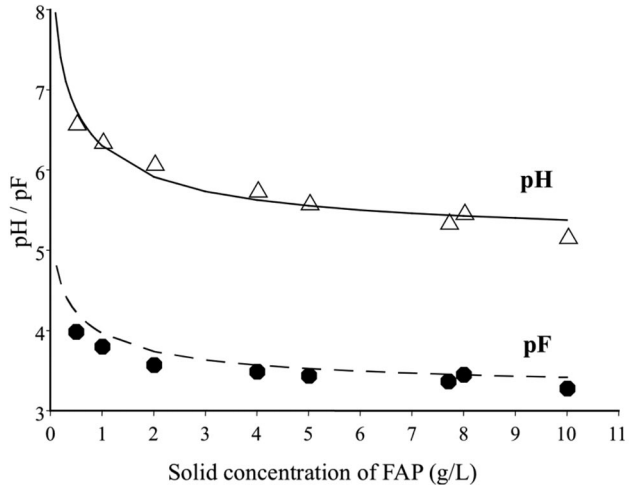

Fig. 4 Simulated and measured pH and pF as a function of the mass of FAP equilibrated in 0.1 M NaCl. (△) and (●) denote the experimental values of pH and pF, respectively. The lines represent the calculated pH and pF values as a function of solid concentration of FAP and are derived using the constants in Table 1. The FAP suspensions were equilibrated for 3.5 months before they were analyzed.

It was found that the calculated pH_{iep} attained a value typical for the HAP system (~8). This can be explained by interpreting reaction 13, which only will result in a decrease in pH as the reaction proceeds to the right, but will not affect the surface charge. However, by assuming a re-adsorption of fluoride ions to the positively charged Ca sites $\equiv CaOH_2^+$, the surface charge will decrease

$$\equiv CaOH_2^+ + F^- \leftrightharpoons \equiv CaF + H_2O \tag{34}$$

Re-adsorption of phosphate ions

With $5 \leq pH \leq pH_0$ both dissolution and surface complexation reactions had to be taken into account. Furthermore, the high Ca/P ratios in solution indicated that there also is re-adsorption of phosphate from the solution to the positively charged surfaces of HAP and FAP (Fig. 5). This observation is in accordance with radioisotope measurements [16]. The re-adsorption probably also occurs at lower pH values, but due to the high concentrations of Ca and phosphate in solution, the effect is not noticeable on the Ca/P ratio in solution. Reaction 35 was included in both models, and the calculations were guided by experimental Ca/P ratios assuming $[Ca^{2+}]_{tot}(sln) = 1.40([P]_{tot}(sln) + [P]_{tot}(srfc)$. This relationship makes it possible to quantify $[P]_{tot}(srfc)$, i.e., the amount of phosphate re-adsorbed. Due to the low specific surface area and lower solubility of FAP, the effect of the re-adsorbed phosphate on Ca/P ratios in solution is small in this system.

$$\equiv CaOH_2^+ + HPO_4^{2-} \leftrightharpoons \equiv CaOPO_3H^- + H_2O \tag{35}$$

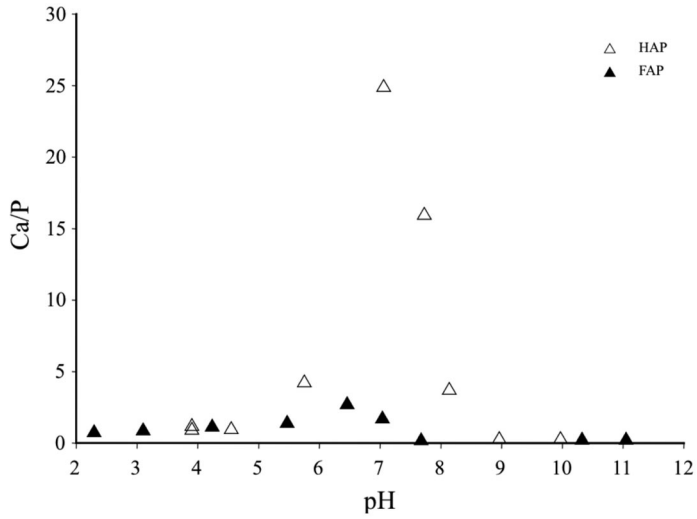

Fig. 5 Experimental Ca/P ratios in solution for (△) HAP and (▲) FAP as a function of pH. The suspensions were equilibrated for 3.5 months in 0.1 M Na(Cl) at 25 °C prior to analysis.

Precipitation of CaF_2

According to the XPS measurements an incongruent dissolution of FAP leading to the formation of CaF_2(s) seems to take place. This assumption is also corroborated by the chemical analysis of Ca and F in solution [13].

The experimental and calculated values for fluoride in solution are depicted together with the calculated amounts of precipitated CaF_2(s) (Fig. 6). The fit between the calculated and experimental data is good assuming a recommended literature value for CaF_2. This fit could be improved by slightly increasing the solubility of CaF_2(s) and the discrepancy could be due to minor errors in the formation constant (which was not optimized in the calculations) but it could also be due to an epitaxial precipitation of CaF_2(s), changing the surface speciation of FAP.

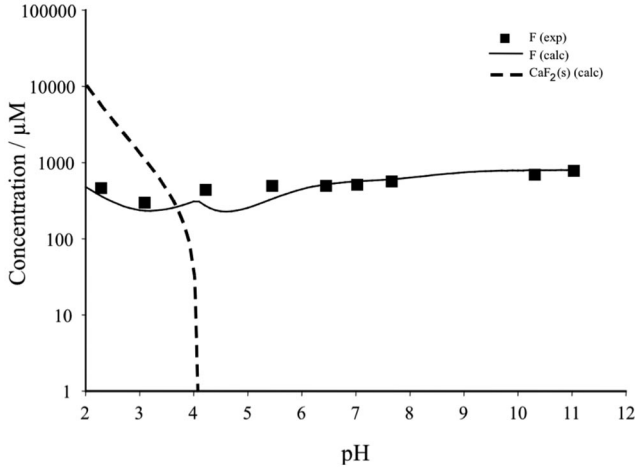

Fig. 6 Calculated amount of CaF_2(s), and experimental and calculated concentrations of fluoride in solution as a function of pH. [FAP] = 7.7 g/l, 0.1 M Na(Cl), T = 25 °C.

FINAL REFINEMENTS

Refined values of the solubility products for HAP and FAP, surface protolytic constants, ion exchange reactions as well as constants for the re-adsorption reactions were refined in calculations in which U(H), U(Ca), U(P), and U(F) were minimized. The final values for the different reactions are found in Table 1. The modeling predictions using the refined values reveal a good agreement between the experimental and calculated data (c.f. Figs. 2, 3, and 6).

The distribution diagrams showing surface speciation of HAP and FAP (Fig. 7) predict positively charged $\equiv CaOH_2^+$ and negatively charged $\equiv OPO_3H^-$ sites over a large pH interval of both apatites. This means that apatite surfaces exhibit zwitterionic properties. It is also clear that the amount of re-adsorbed phosphate is higher on the HAP surface compared to the FAP surface, which is in accordance with previous discussions on the differences in solubility and specific surface area between the two minerals. It can also be noted that channels of the structure in which ≡F and/or ≡OH reside show ion exchange properties in which ≡F predominates with pH < 5. At higher pH values the surface speciation of FAP changes to become increasingly similar to the surface speciation of HAP.

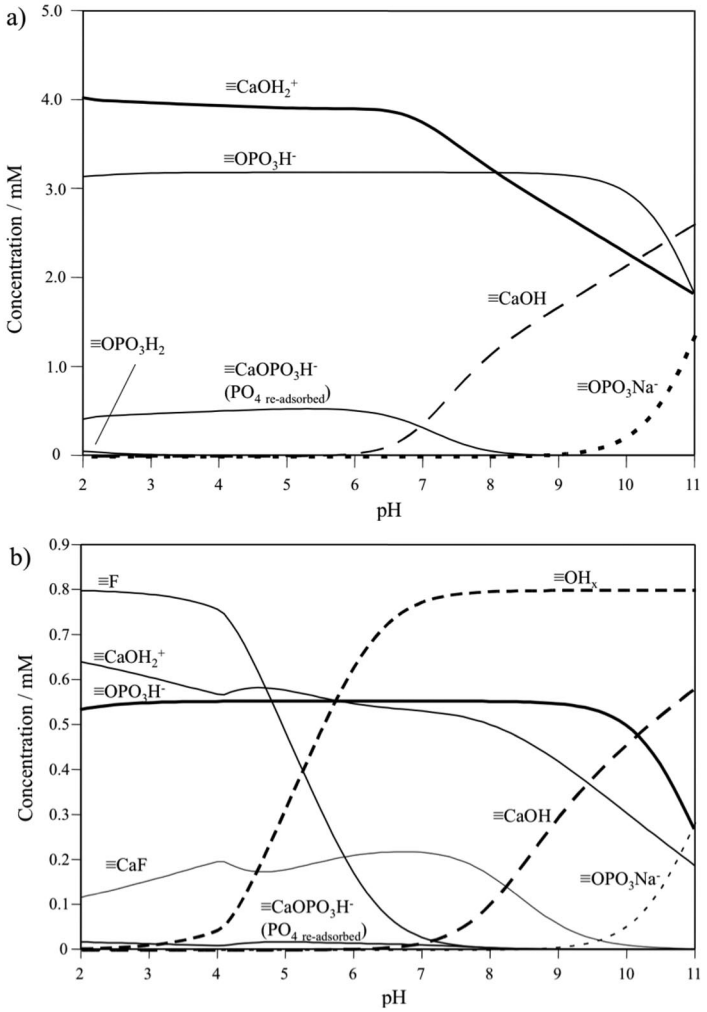

Fig. 7 Calculated surface speciation of (a) HAP and (b) FAP as a function of pH, in I = 0.1 M Na(Cl), and at T = 25 °C and a solid concentration of 7.7 g/l.

Finally, the calculated values of the surface potentials including all above-mentioned surface reactions resulted in $\Psi = 0$ mV with pH = 7.9 for HAP and 5.3 for FAP. These values are in good agreement with pH_{iep} = 8.1 for HAP and pH_{iep} = 5.7 for FAP obtained from the electrophoretic mobility measurements.

CONCLUSIONS

It has been shown that the dissolution processes are very complex, and the approach throughout this study has, therefore, been to quantitatively measure and interpret not only the dissolution products in solution and adsorption/desorption processes at the mineral surfaces, but also using spectroscopic techniques to find out how the different experimental conditions affect the surfaces chemistry of the minerals.

One of the most important findings was that both apatites had formed surface layers different than the bulk when they were equilibrated in aqueous solutions. As the surface governs the solubility of a mineral, it was of great importance to find out the composition of the surface before performing additional experiments on these minerals. Batch experiments, potentiometric titrations together with XPS and ATR-FTIR measurements provided the information required to calculate thermodynamic models for the dissolution reactions of the two apatites. The modeling efforts also gave insight into the surface speciation in terms of surface protonation/deprotonation reactions, the ion exchange process between surface fluoride ions, and hydroxide ions of the bulk solution as well as readsorption reactions involving phosphate and fluoride ions. The latter process is probably partially responsible for the lower solubility of FAP as the fluoride ions released from the FAP surface during dissolution becomes re-adsorbed to positively charged Ca sites, thereby stabilizing the FAP surface. The resulting model also corroborates observations from XPS and solubility data, claiming the formation of CaF_2(s) in the most acidic pH range of the FAP system. Finally, calculated isoelectric points (pH_{iep}) are in agreement with values from surface charge measurements showing pH_{iep} (HAP) = 8.1 and pH_{iep} (FAP) = 5.7.

ACKNOWLEDGMENTS

This work was supported by the Swedish Research Council and Georange. The Kempe Foundation, Sweden, is acknowledged for funding of the FTIR spectrometer, and the Wallenberg Foundation, Sweden, for funding the XPS instrument.

REFERENCES

1. G. M. Filippelli. *Phosphates: Geochemical, Geobiological, and Materials Importance*, Vol. 48, M. J. Kohn, J. Rakovan, J. M. Hughes (Eds.), Mineralogical Society of America (2002).
2. R. McDowell, S. Sinjaj, A. Sharpley, E. Frossard. *Soil Sci.* **166**, 365 (2001).
3. P. H. Moisander, T. F. Steppe, N. S. Hall, J. Kuparinen, H. W. Paerl. *Mar. Ecol. Progr. Rep. Ser.* **262**, 81 (2003).
4. E. O. Oelkers, E. Valsami-Jones. *Elements* **2**, 83 (2008).
5. D. L. Jones. *Plant Soil* **205**, 25 (1998).
6. K. A. Gross, C. C. Berndt. In *Phosphates: Geochemical, Geobiological, and Materials Importance*, Vol. 48, M. J. Kohn, J. Rakovan, J. M. Hughes (Eds.), pp. 631–672, Mineralogical Society of America (2002).
7. J. C. Elliot. In *Phosphates: Geochemical, Geobiological, and Materials Importance*, Vol. 48, M. J. Kohn, J. Rakovan, J. M. Hughes (Eds.), pp. 427–453, Mineralogical Society of America (2002).
8. M. J. Dallemagne, L. J. Richelle. In *Biological Mineralization*, Vols. 23–42, I. Zipkin (Ed.), John Wiley, New York (1973).

9. D. N. Misra. *J. Biomed. Mater. Res.* **48**, 848 (1999).
10. W. E. Brown, T. M. Gregory L. C. Chow. *Caries Res.* **11**, 118 (1977).
11. S. K. Doss. *J. Dent. Res.* **5**, 1067 (1976).
12. Å. Bengtsson, A. Shchukarev, P. Persson, S. Sjöberg. *Geochim. Cosmochim. Acta* **73**, 257 (2009).
13. Å. Bengtsson, A Shchukarev, P. Persson, S. Sjöberg. *Langmuir* **25**, 2355 (2009).
14. E. Hayek, W. Stadlmann. *Angew. Chem.* **67**, 327 (1955).
15. G. Penel, G. Leroy, C. Rey, B. Sombret, J. P. Huvenne, E. Bres. *J. Mater. Sci.: Mater. Med.* **8**, 271 (1997).
16. M. Kukura, L. C. Bell, A. M. Posner, J. P. Quirk. *J. Phys. Chem.* **76**, 900 (1972).
17. P. W. Brown, R. I. Martin. *J. Phys. Chem.* **103**, 1671 (1999).
18. C. Park, P. Fenter, Z. Zhang, L. Cheng, N. C. Sturchio. *Am. Mineral.* **89**, 1647 (2004).
19. E. E. Berry. *J. Nucl. Chem.* **29**, 317 (1967).
20. J. L. Meyer, B. O. Fowler. *Inorg. Chem.* **21**, 3029 (1982).
21. M. Jarlbring, D. E. Sandström, O. N. Antzutkin, W. Forsling. *Langmuir* **22**, 4787 (2006).
22. D. E. Sandström, M. Jarlbring, O. N. Antzutkin, W. Forsling. *Langmuir* **22**, 11060 (2006).
23. S. K. Doss. *J. Dent. Res.* **5**, 1067 (1976).
24. L. C. Bell, A. M. Posner, J. P. Quirk. *J. Colloid Interface Sci.* **42**, 250 (1973).
25. M. Jarlbring, L. Gunneriusson, W. Forsling. *J. Colloid Interface Sci.* **285**, 206 (2005).
26. J. Perrone, B. Fourest, E. Giffaut. *J. Colloid Interface Sci.* **249**, 441 (2002).
27. P. W. Schindler, H. Gamsjäger. *Kolloid Z. Z. Polym.* **250**, 759 (1972).
28. M. K. Ridley, M. L. Machesky, D. J. Wesolowlski, D. A. Palmer. *Geochim. Cosmochim. Acta* **68**, 239 (1997).
29. R. P. J. J. Rietra, T. Hiemstra, W. H. Van Riemsdijk. *Environ. Sci. Technol.* **35**, 3369 (2001).
30. J. S. Geelhoed, T. Hiemstra, W. H. van Riemsdijk. *Geochim. Cosmochim. Acta* **61**, 2389 (2004).
31. E. Laiti, P. Persson, L. O. Öhman. *Langmuir* **12**, 2969 (1996).
32. R. Strauss, G. W. Brümmer, N. J. Barrow. *Eur. J. Soil Sci.* **48**, 101 (1997).
33. R. M. Smith, A. E. Martell. *Critical Stability Constants, VI: Second Supplement*, Plenum (1989).
34. C. W. Davis. *Ion Association*, Butterworth (1962).
35. M. Karlsson, J. Lindgren. <http://www.dagger.mine.nu/MAJO/winsgw.htm> (2006).
36. G. Eriksson. *Anal. Chim. Acta* **112**, 375 (1979).